

Structural evolution and medium-temperature thermochronology of central Madagascar: implications for Gondwana amalgamation

Sheree E. Armistead^{a,b,c*}, Alan S. Collins^a, Ahmad Redaa^{a,d}, Gilby Jepson^{a,e}, Jack Gillespie^{a,f}, Sarah Gilbert^g, Morgan L. Blades^a, John D. Foden^a, Théodore Razakamanana^h

^aTectonics & Earth Systems Research Group, Mawson Centre for Geoscience, Department of Earth Sciences, University of Adelaide, SA, Australia

^bGeological Survey of Canada, 601 Booth Street, Ottawa, Ontario, Canada

^cMetal Earth, Harquail School of Earth Sciences, Laurentian University, Sudbury, Ontario, Canada

^dFaculty of Earth Sciences, King Abdulaziz University, Jeddah, Saudi Arabia

^eDepartment of Geosciences, University of Arizona, 1040 E. 4th Street, Tucson, Arizona, USA

^fThe Institute for Geoscience Research (TIGeR), School of Earth and Planetary Sciences, Curtin University, Perth, Australia

^gAdelaide Microscopy, University of Adelaide, Adelaide, SA, Australia

^hDépartement des Sciences de la Terre, Université de Toliara, Toliara, Madagascar

*correspondence (sheree.armistead@adelaide.edu.au)

This manuscript has been accepted in the JOURNAL OF THE GEOLOGICAL SOCIETY.

Previous versions of this manuscript are available at doi.org/10.31223/osf.io/x46vc

Version history:

Version 1: Submitted 18th December 2018;
Rejected with invitation to resubmit 11th March 2019 ☹

Version 2: Submitted 19th August 2019;
Major revision returned 19th October 2019 ☺

Version 3: Revised submission 16th December 2019;
Minor revisions returned 15th January 2020;
Revised submission 28th January 2020;
ACCEPTED 1st February 2020 !! ☺ ☺

1 Abstract

2 Madagascar occupied an important place in the amalgamation of Gondwana and preserves a record of
3 several Neoproterozoic events that are linked to orogenesis of the East African Orogen. In this study, we
4 integrate remote sensing, field data and thermochronology to unravel complex deformation in the
5 Ikalamavony and Itremo domains of central Madagascar. The deformation sequence comprises a
6 gneissic foliation (S1), followed by south to south-west directed, tight to isoclinal, recumbent folding
7 (D2). These are overprinted by north-trending upright folds that formed during an ~E-W shortening
8 event (D3). Together these produced type 1 and type 2 fold interference patterns throughout the
9 Itremo and Ikalamavony domains. We show that the Itremo and Ikalamavony domains were deformed
10 together in the same orogenic system, which we interpret as the c. 630 Ma collision of Azania with
11 Africa along the Vohibory Suture in southwestern Madagascar. In eastern Madagascar, deformation is
12 syn- to post-550 Ma, which likely formed in response to final closure of the Mozambique Ocean along
13 the Betsimisaraka Suture that amalgamated Madagascar with the Dharwar Craton of India. Apatite U-
14 Pb and novel LA-QQQ-ICP-MS muscovite and biotite Rb-Sr thermochronology indicate that much of
15 central Madagascar cooled through ~500°C at c. 500 Ma.

16 **Keywords:** thermochronology, Gondwana, remote sensing, GIS, supercontinents

17 **Supplementary material:**

18 Supplementary A: Detailed geological map of central Madagascar

19 Supplementary B: Detailed methodology and geo/thermochronology results

20 Supplementary C: Isotopic data for geo/thermochronology

21 Supplementary D: Landsat images and structural interpretation examples

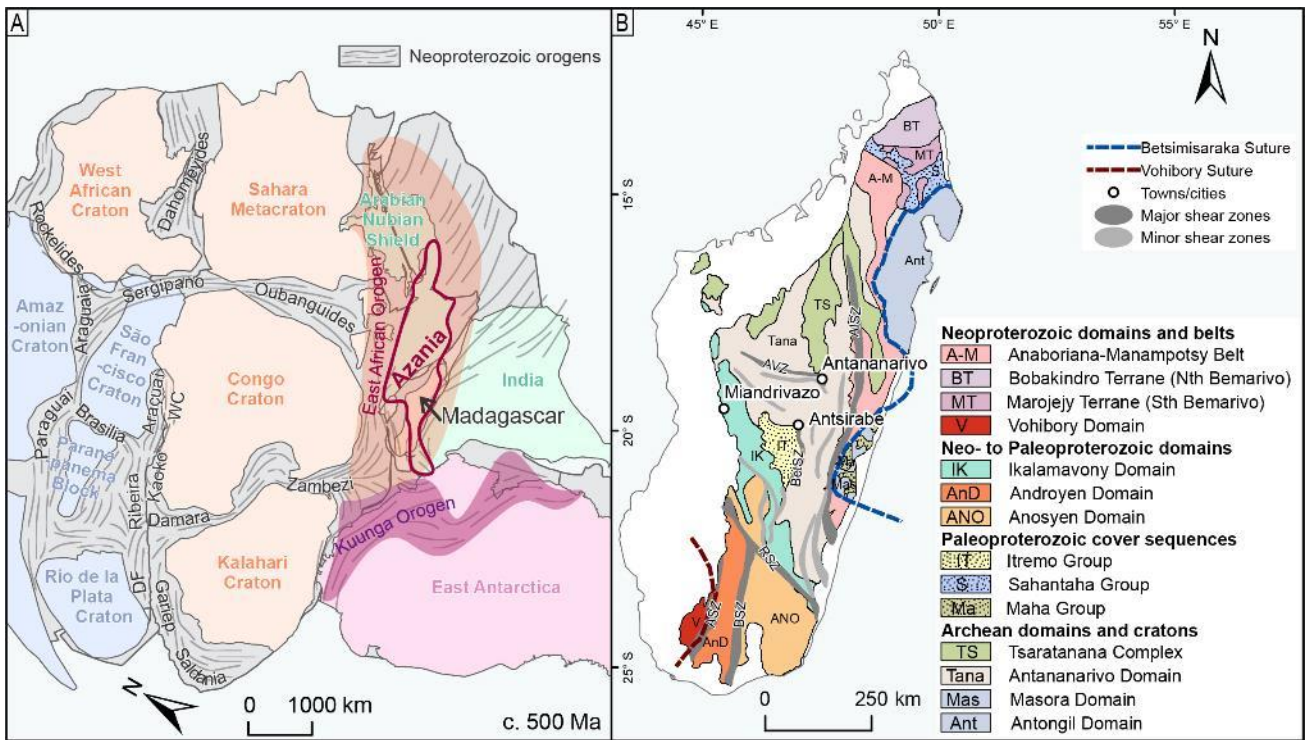
22 1. Introduction

23 The amalgamation of central Gondwana occurred through convergence at several discrete subduction
24 and collisional zones; collectively forming the East African Orogen. Madagascar was located in the
25 centre of Gondwana and provides an ideal natural laboratory to study how this supercontinent
26 coalesced (Figure 1a) (Collins, 2006; Collins and Windley, 2002; Tucker et al., 1999). Of particular
27 interest and contention, is how and when the Archean nucleus of Madagascar amalgamated with the
28 Dharwar Craton of India to the east, and East Africa to the west, as well as smaller continental blocks of
29 equivocal origin. Reconciling this tectonic history has major implications for global plate tectonic
30 models of the Neoproterozoic (e.g. Merdith et al., 2017).

31 Central Madagascar comprises the Archean Antananarivo Domain, the Proterozoic Itremo sub-domain
32 and the Neoproterozoic Ikalamavony Domain. These terranes are bound by two postulated major
33 sutures; the eastern Betsimisaraka Suture and the western Vohibory Suture (mapped as the Ampanihy
34 shear zone in Figure 1b). These sutures resulted from at least two distinct orogenic events that
35 amalgamated central Madagascar, the Dharwar Craton of India, and Africa within Gondwana (Figure

36 1a). However, the timing, location, and direction of subduction leading to these orogenic events
 37 remain contentious. Two end-member models are generally evaluated for the amalgamation of
 38 Madagascar; 1) that the Dharwar–central Madagascar collision (eastern suture) occurred in the late
 39 Archean, and that central Madagascar and the Dharwar craton existed as the “Greater Dharwar Craton”
 40 through the entire Proterozoic eon (Tucker et al., 2011), and that widespread Neoproterozoic–
 41 Cambrian magmatism and metamorphism in Madagascar resulted from Madagascar–Africa collision
 42 (western suture); or 2) that the Dharwar Craton and central Madagascar were separate terranes that
 43 were sutured during a major Ediacaran–Cambrian East African orogenic event (the Malagasy Orogeny
 44 of Collins and Pisarevsky 2005), marked by the Betsimisaraka Suture in eastern Madagascar (Figure
 45 1b). An age of c. 750–650 Ma for this suture has alternatively been proposed (Fitzsimons and Hulscher,
 46 2005). Several authors have proposed that the central Madagascar–Africa collision occurred at c. 650–
 47 630 Ma (Collins and Pisarevsky, 2005; Collins and Windley, 2002; Emmel et al., 2008; Horton et al.,
 48 2016; Jöns and Schenk, 2011). Other authors have suggested a c. 850–750 Ma age for a suture in
 49 western Madagascar (Moine et al., 2014). The proximity of these two suture zones makes it difficult to
 50 unravel the timing of events, as more recent events have obscured the record of earlier events through
 51 high temperature resetting of key minerals used for thermochronology and metamorphism.

52



53

54 Figure 1 a) Tectonic map of Gondwana made using GPlates exported geometries from Merdith et al. (2017) in ArcGIS;
 55 projected in Hotine Oblique Mercator with Madagascar in the centre (reconstructed position, longitude=-75° and
 56 latitude=+40°). DF=Dom Feliciano Belt, WC=West Congo; b) Present day map of the geological domains of Madagascar after
 57 De Waele et al. (2011). AISZ=Angavo-Ifanadiana shear zone, AVZ=Antananarivo virgation zone, BetSZ=Betsileo shear zone,
 58 RSZ=Ranotsara shear zone, BSZ=Beraketa shear zone, ASZ=Ampanihy shear zone.

59 1.1. Regional geology

60 Madagascar is made up of several domains ranging in age from Archean to Neoproterozoic (Figure 1b).
61 The centre of Madagascar is made up of the Antananarivo Domain, which has a basement of c. 2500
62 Ma magmatic gneisses (Collins and Windley, 2002; Kröner et al., 2000; Tucker et al., 1999), known as
63 the Betsiboka Suite (Roig et al., 2012), interleaved with the Ambatolampy Group granulite- and
64 amphibolite-facies metasedimentary rocks (Archibald et al., 2015). To the east of the Antananarivo
65 Domain is the Antongil-Masora Domain, which contains gneisses that are c. 3100 Ma and c. 2500 Ma,
66 and are interpreted as a continuation of the Dharwar Craton of India (Armistead et al., 2017; Schofield
67 et al., 2010; Tucker et al., 1999).

68 Overlying the Antananarivo Domain is the Itremo Group (Figure 1b; Figure 2). Classified as a sub-
69 domain of the Antananarivo Domain by Roig et al. (2012), the Itremo Group is comprised of
70 quartzites, schists and marbles with a maximum depositional age of c. 1600 Ma (Cox et al., 1998;
71 Fernandez et al., 2003). The Itremo Group is interpreted as a continental margin sequence that was
72 deposited on the Antananarivo Domain basement (Cox et al., 1998; 2004). The Itremo nappes in the
73 Itremo Domain have been investigated extensively due to their prominence in remotely sensed data
74 and availability of outcrops (Collins et al., 2003b; Tucker et al., 2007).

75 To the southwest, thrust over the Itremo Group, is the Ikalamavony Group within the Ikalamavony
76 Domain, similarly made up of quartzites, schists and marbles but with a maximum depositional age of
77 c. 1000 Ma (Archibald et al., 2017a; Tucker et al., 2014). In places the Ikalamavony Domain is in
78 tectonic contact directly with the Antananarivo Domain basement, with no Itremo Group rocks
79 separating them (Figure 1b; Figure 2). Unique to the Ikalamavony Domain is the c. 1000 Ma Dabolava
80 Suite, which is composed of granitic to gabbroic orthogneiss (Archibald et al., 2017a). The Dabolava
81 Suite and the age-equivalent Ikalamavony Group have been interpreted as an oceanic arc terrane
82 (Archibald et al., 2017a). This terrane must have accreted prior to the intrusion of the c. 850–750 Ma
83 Imorona-Itsindro Suite, which intrudes the Ikalamavony, Itremo and Antananarivo domains—placing a
84 minimum age on the juxtaposition of the three central Madagascan domains. The relationship between
85 the Ikalamavony Domain and the Itremo Group remains poorly understood, and is the focus of this
86 study.

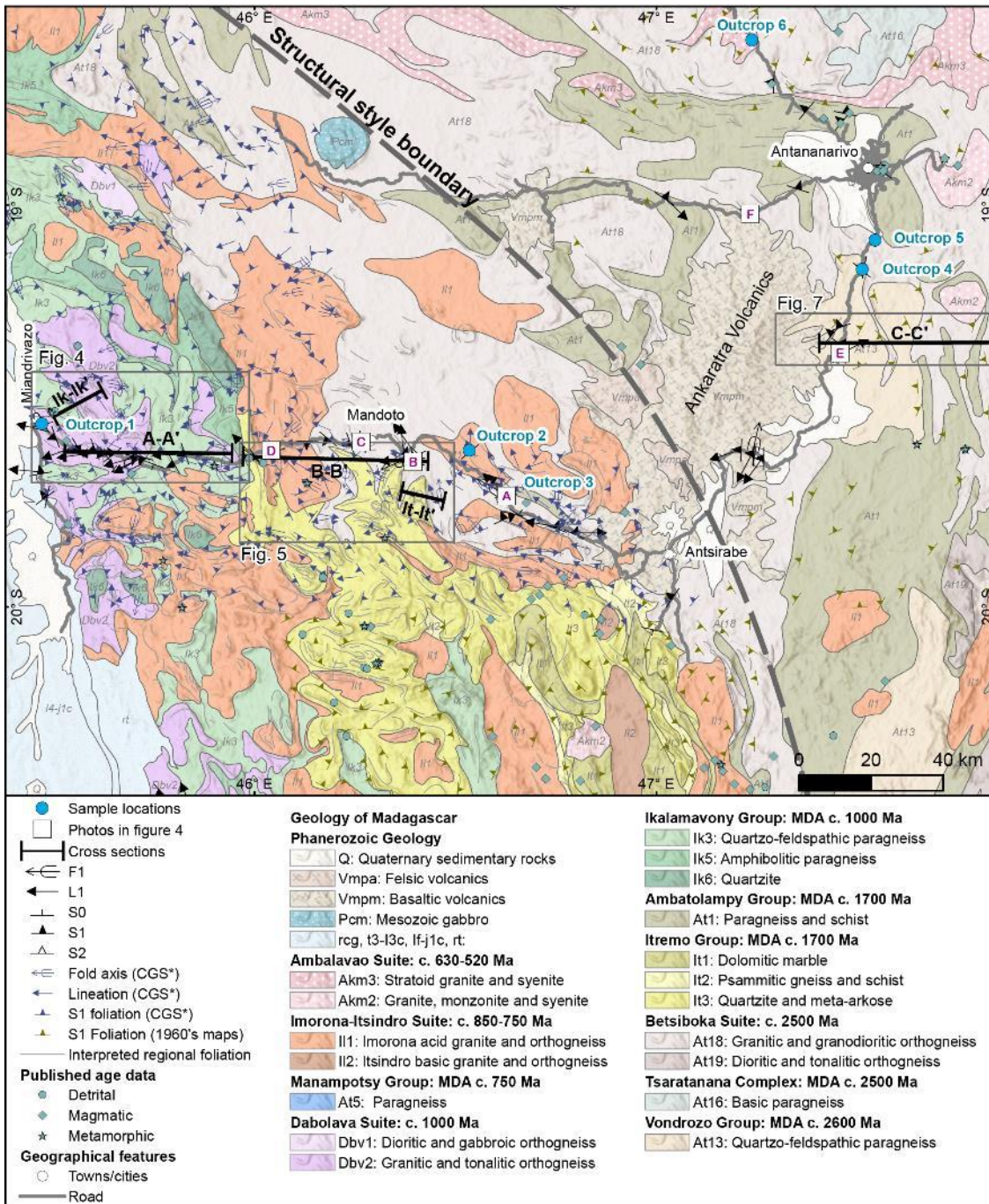
87 To the south of these metasedimentary terranes are the Proterozoic Anosyen, Androyen and Vohibory
88 domains (Boger et al., 2014; de Wit et al., 2001; Emmel et al., 2008; Horton et al., 2016; Jöns and
89 Schenk, 2008). In northern Madagascar is the c. 800–700 Ma Bemarivo Domain, which formed as an
90 exotic juvenile arc terrane that amalgamated with Madagascar at c. 520 Ma, possibly in relation to the
91 Betsimisaraka Suture (Armistead et al., 2019; Jöns et al., 2009; Thomas et al., 2009).

92 1.2. Regional structural and geochronological framework for central Madagascar

93 This study focuses on central Madagascar including parts of the Ikalamavony, and Antananarivo
94 domains and the Itremo sub-domain (Figure 1b, Figure 2). The structural relationships between these
95 domains has not yet been studied in detail. We use structural geology and various geochronological
96 methods to define and distinguish deformation events in central Madagascar. Collins et al. (2003b) and

97 Tucker et al. (2007) undertook comprehensive studies of the structure of the Itremo Group in central
98 Madagascar. This area contains spectacularly folded sequences visible from satellite imagery. Collins et
99 al. (2003b) interpreted a D1 event that produced 10 km scale recumbent, isoclinal folding predating c.
100 800–780 Ma intrusive rocks of the Imorona-Itsindro Suite. D2 was interpreted as a local deformation
101 event that occurred synchronously with c. 800–780 Ma intrusions. D3 was interpreted as an east-west
102 shortening event with thrusting and at least two phases of upright folding. D4 is expressed as post-550
103 Ma normal shearing and locally marks the boundary between the least metamorphosed parts of the
104 Itremo Group and the granulite-facies Betsiboka Suite and Ambatolampy Group of the Antananarivo
105 Domain (Betsileo Shear Zone; Figure 1b; Collins et al. 2000). Tucker et al. (2007) interpreted a similar
106 history for the Itremo Group with km-scale fold and thrust nappes, and east-directed vergence. This
107 resulted in inversion and repetition of the Archean Antananarivo Domain gneisses and the Proterozoic
108 Itremo Group, with high-grade (old) rocks being thrust over low-grade (young) rocks. The inversion
109 was followed by east-west shortening that resulted in upright folding of nappes to produce km-scale
110 fold interference patterns. This shortening event occurred within a sinistral transpressive regime and
111 was interpreted as being associated with the Ranotsara Shear Zone (Figure 1b) in southern Madagascar
112 (Tucker et al., 2007). Although these models are similar in their sequence and style of deformation,
113 they differ in that Tucker et al. (2007) interpreted the timing of deformation as occurring after c. 720
114 Ma, whereas Collins et al. (2003b) interpreted the early nappes as forming before 800–780 Ma, and the
115 upright folding having occurred after the c. 780 Ma intrusive rocks.

116 The region between the eastern-most part of our study area and the east coast of Madagascar
117 (approximately the location of the Betsimisaraka Suture in Figure 1b) was studied from a structural
118 perspective in Collins et al. (2003a); Martelat et al. (2000); Nédélec et al. (2000); Raharimahefa and
119 Kusky (2006); Raharimahefa and Kusky (2009); Raharimahefa et al. (2013). Interpretations of this
120 region generally include a D1 event characterised by N-S striking foliations that dip to the west, with a
121 top to the east sense of movement (Collins et al., 2003a; Nédélec et al., 2000). These rocks are reworked
122 by D2 shear zones such as the Angavo Shear Zone and the Antananarivo virgation zone (Figure 1b) that
123 underwent low-pressure, granulite conditions (Nédélec et al., 2000; Paquette and Nédélec, 1998). D3
124 is characterised by >20 km wide mylonitic high-strain zones and smaller discrete shear zones (Collins
125 et al., 2003a). These dip gently to the west, with a top to the east sense of movement. D4 is
126 characterised by poorly preserved late stage folding (Collins et al., 2003a). A syn-kinematic granite
127 within the Angavo Shear Zone constrains deformation here to c. 550 Ma (Raharimahefa and Kusky,
128 2010).



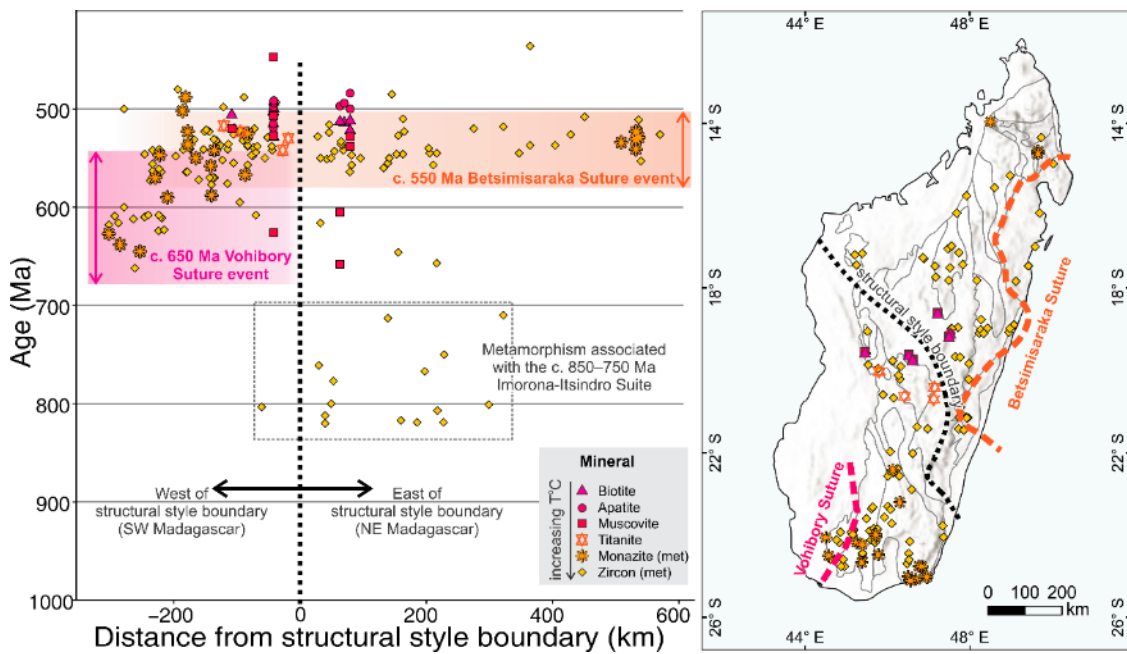
129

130 Figure 2 Geological map of central Madagascar (Roig et al., 2012) with sample locations, photo locations from Figure 6, our
 131 remote sensing interpretation, new structural measurements and structural measurements from Macey et al. (2009); Moine
 132 (1968); Service Géologique de Madagascar (1962); Service Géologique de Madagascar (1963a); Service Géologique de
 133 Madagascar (1963b), and published geochronology. Numbers associated with these points are provided in a detailed PDF
 134 copy of this map where layers can be turned on and off, and further information obtained from the model tree in a pdf
 135 viewer (Supplementary A).

136 Precise dating of deformation in Madagascar is difficult due to resetting from successive overlapping
 137 thermo-tectonic events. Latest metamorphism in the Anosyen and Androyen domains to the south of
 138 our study area is constrained to c. 580–520 Ma (Figure 3) (Collins et al., 2012; de Wit et al., 2001;
 139 Martelat et al., 2000; Paquette et al., 1994) and attributed to high-strain shearing along the Ampanihy
 140 and Beraketa shear zones (Figure 1b) (Boger et al., 2015; Boger et al., 2014). Horton et al. (2016); Jöns

141 and Schenk (2011) demonstrated that in southern Madagascar, high-grade metamorphism yielded
 142 ages of c. 650–600 Ma west of the Vohibory Suture (Figure 3), but recorded ages of c. 560–530 Ma to
 143 the east of this suture. In central Madagascar, U–Pb dating of zircon rims and titanite have been used
 144 to constrain latest metamorphism in the Itremo Group to c. 550–500 Ma (Tucker et al., 2007). Further
 145 east, between the eastern-most part of the study area and the east coast of Madagascar, metamorphism
 146 has been dated to c. 560–520 Ma (BGS-USGS-GLW, 2008; Collins et al., 2003c; Kröner et al., 2000).
 147 From this, it is clear that whatever event was taking place at c. 580–520 Ma, its effects were widespread
 148 and resulted in metamorphism throughout most of Madagascar, sparing, perhaps, the far southwest.

149 The cross-cutting relationships and deformation history of the rocks within the terranes that make up
 150 Madagascar can provide clues as to the timing of major orogenic events. Here we use structural geology
 151 to understand the deformation history of a poorly understood part of central Madagascar, which lies
 152 between the two hypothesised suture zones. We attempt to link up previous structural studies and
 153 further extend these interpretations to cover the entire central Madagascar region. We have used
 154 remotely sensed data such as satellite imagery and Landsat to interpret the structural framework of
 155 central Madagascar, and integrated existing geochronological and structural data (Supplementary A).
 156 We have ground-truthed this interpretation by collecting structural data and key rock samples for U–
 157 Pb zircon, U–Pb apatite, Rb–Sr muscovite and Rb–Sr biotite analysis (Supplementary B; Supplementary
 158 C). Rb–Sr mica laser ablation QQQ-ICP-MS dating in particular is a novel technique and this research
 159 represents some of the first published ages using this technique. These isotopic systems span a wide
 160 range of closure temperatures from which we can reconstruct the temporal and thermal evolution of
 161 this region.



162
 163 Figure 3 Summary of published metamorphic data for Madagascar and new data collected in this study. Biotite, apatite and
 164 muscovite are from this study. Metamorphic minerals zircon, monazite and titanite are from the compilation of Tucker et al.
 165 (2014). Locations of data points shown in the map to the right, terranes are the same as those from Figure 1b.

166 2. Structure of central Madagascar

167 Large-scale structures, fold interference patterns, faults and shear zones are recognisable in remotely
168 sensed data in the region west of Antsirabe (Figure 2). Examples of Landsat images used for
169 interpretation are presented in Supplementary D. East of Antsirabe, polydeformed folds are not
170 observed and the structural style changes significantly. We have delineated this as a 'structural style
171 boundary' in Figure 2. Here we further extend previous interpretations of the Itremo sub-domain
172 (Collins et al., 2003b; Tucker et al., 2007) to the Ikalamavony Domain, where identification of
173 lithostratigraphy from remotely sensed data is more difficult, and interpretation is less straightforward.

174 2.1. Ikalamavony Domain

175 The Ikalamavony Domain contains metasedimentary rocks of the Ikalamavony Group, which are
176 dominated by paragneiss, schist, quartzite and amphibolite (Figure 4). We observe many of the
177 gneisses with bands of mylonite, indicating a high strain environment. Based on remote sensing data,
178 we interpret a thrust fault separating the Ikalamavony Domain and Itremo sub-domain (Figure 5). This
179 fault is interpreted based on the sharp contrast in lithologies and the linear nature of the fault observed
180 in remote sensing data. Due to the scarcity of fresh outcrop, we were unable to observe this fault in the
181 field, however rocks were more strongly deformed in this area.

182 2.1.1. *D1 Deformation*

183 The first recognisable deformation event at the outcrop scale is defined by a pervasive foliation
184 observed in orthogneisses, paragneisses and metasedimentary rocks. In orthogneisses and
185 paragneisses, the foliation is typically defined by the elongation and alignment of biotite, feldspar and
186 quartz. In metasedimentary rocks such as schist and paragneiss, the foliation is commonly defined by
187 the orientation of biotite crystals and biotite rich layers. Primary sedimentary features such as bedding
188 were difficult to recognise due to significant metamorphism and recrystallisation.

189 In remotely sensed data, linear or curvilinear trends such as ridges, are interpreted as being
190 representative of the S1 foliation. Quartzite units in particular, which are less common than in the
191 Itremo sub-domain, are easy to recognise in remotely sensed data due to the large contrast in different
192 Landsat bands (e.g. Supplementary D). In the Ikalamavony Domain the orientation of measured S1
193 foliations is dominantly northwest trending, and lineations and fold axes plunge moderately toward the
194 west.

195 2.1.2. *D2 Deformation*

196 D2 deformation is most easily identifiable from remotely sensed data due to the large scale (>1 km)
197 wavelength folds. F2 antiforms and synforms are identifiable by the repetition of mapped geological
198 units and constrained by structural measurements (Figure 4). D2 is defined by tight to isoclinal folds
199 with axial traces approximately parallel to S1 in fold limbs. At the outcrop scale we observe these as
200 decimetre- to metre-scale asymmetric, tight to isoclinal folds. F2 folds are similar-type folds, with
201 thickened hinge zones and thinned limbs. An axial planar foliation is difficult to recognise in outcrops,
202 but sometimes occurs as the alignment of biotite in hinge zones. Due to the isoclinal nature of folding,

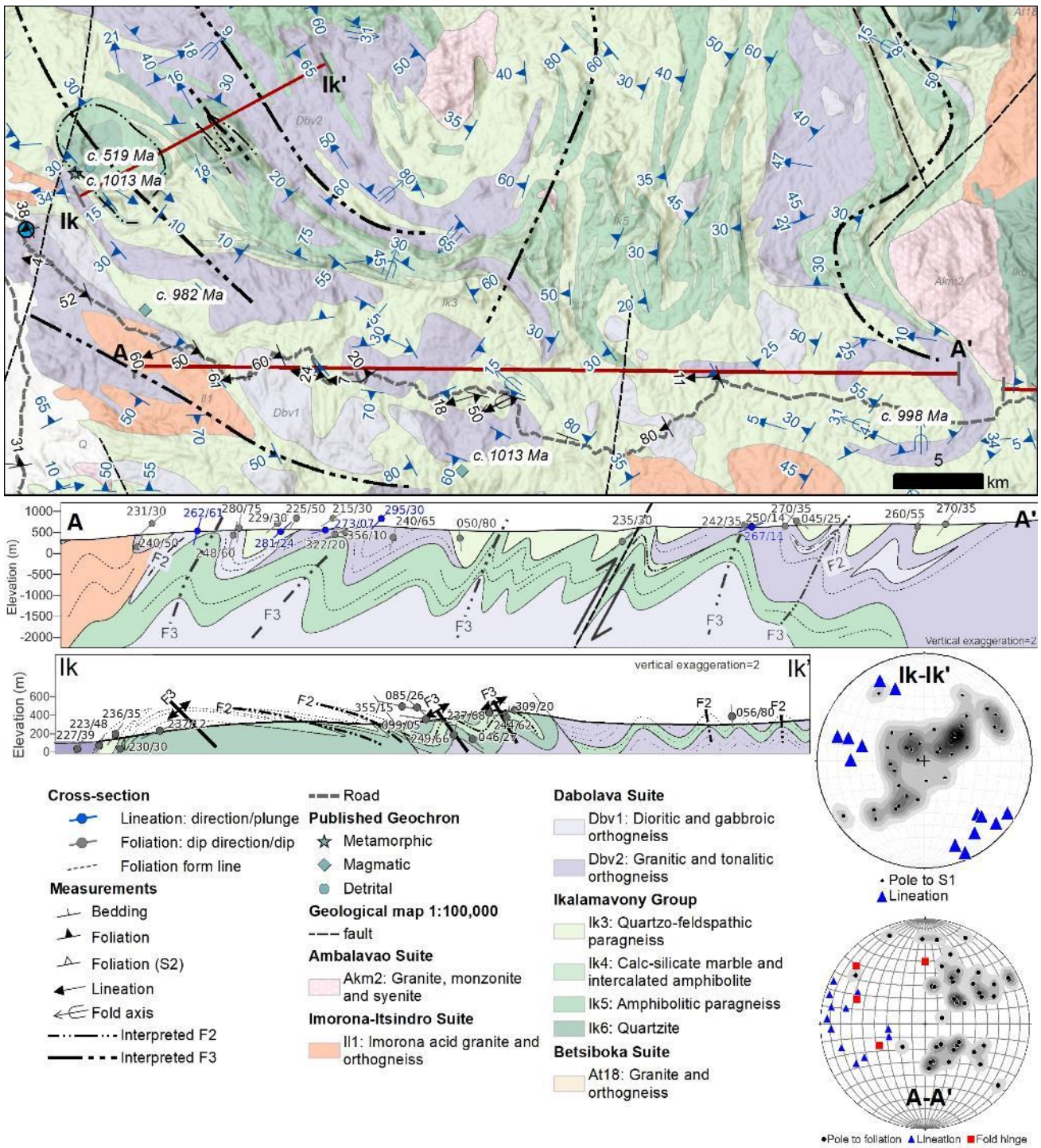
203 F2 axial traces are approximately parallel to S1 at the regional scale. F2 folds would have formed with
204 axial traces striking ~east-west, however due to subsequent deformation during D3 and D4, they are
205 now preserved with variable orientations.

206 *2.1.3. D3 Deformation and associated fold interference patterns*

207 We do not observe evidence for a third generation deformation event at the outcrop scale, however D3
208 folds are recognisable in remotely sensed data. The folding of F2 folds during D3 has produced a series
209 of fold interference patterns. Type 1 and type 2 fold interference patterns are observed in remotely
210 sensed data (Figure 4; Figure 5). Type 1 folds occur when an upright folding event is overprinted by an
211 orthogonal upright folding event (Grasemann et al., 2004) and is expressed in Supplementary D(b).
212 Type 2 fold interference patterns occur when a recumbent folding event is orthogonally overprinted by
213 an upright folding event (Grasemann et al., 2004) and is expressed in Figure 5. We interpret D3 as the
214 result of ~northeast-southwest shortening (present day orientation). Cross-section Ik-Ik' (Figure 4)
215 has F2 folds that are very tight to isoclinal, with axial traces approximately parallel to F3 in F3 fold
216 limbs. This formed by ~southeast-directed recumbent folding that was overprinted by a north to
217 northwest trending F3 fold.

218 *2.1.4. D4 Deformation*

219 The axial traces of F3 folds vary across the Ikalamavony Domain, indicating a fourth generation of
220 deformation. For example the F3 fold axes vary from northwest-trending in the west near Miandrivazo
221 (e.g. Ik-Ik' cross-section in Figure 4), and curve to become north- to northeast-trending in the centre of
222 the map in Figure 4. We suggest this is caused by large wavelength (~30–50 km), F4 open folding with
223 approximately east-west shortening.



224

225 Figure 4 Geological map, structural data and cross-sections through the Ikalamavony Domain using both our new data
 226 (black) and previously published data (blue) (Macey et al., 2009). Fold axis measurements are generally interpreted to be F2
 227 folds since we do not observe any overprinting fold generations in the field. A-A' shows the overall trend of structures in the
 228 Ikalamavony Domain. Ik-Ik': an example of type 2 fold interference patterns with north-west trending third generation
 229 upright folds. Sections generated using QProf plugin in QGIS. Structural measurements (dip direction/dip) within ~2km of
 230 the section are projected along the profile. Topographic profile derived from 30 arc-second DEM of Africa (USGS).
 231 Geological polygons from Council for Geosciences 1:100000 mapsheets (Macey et al., 2010).

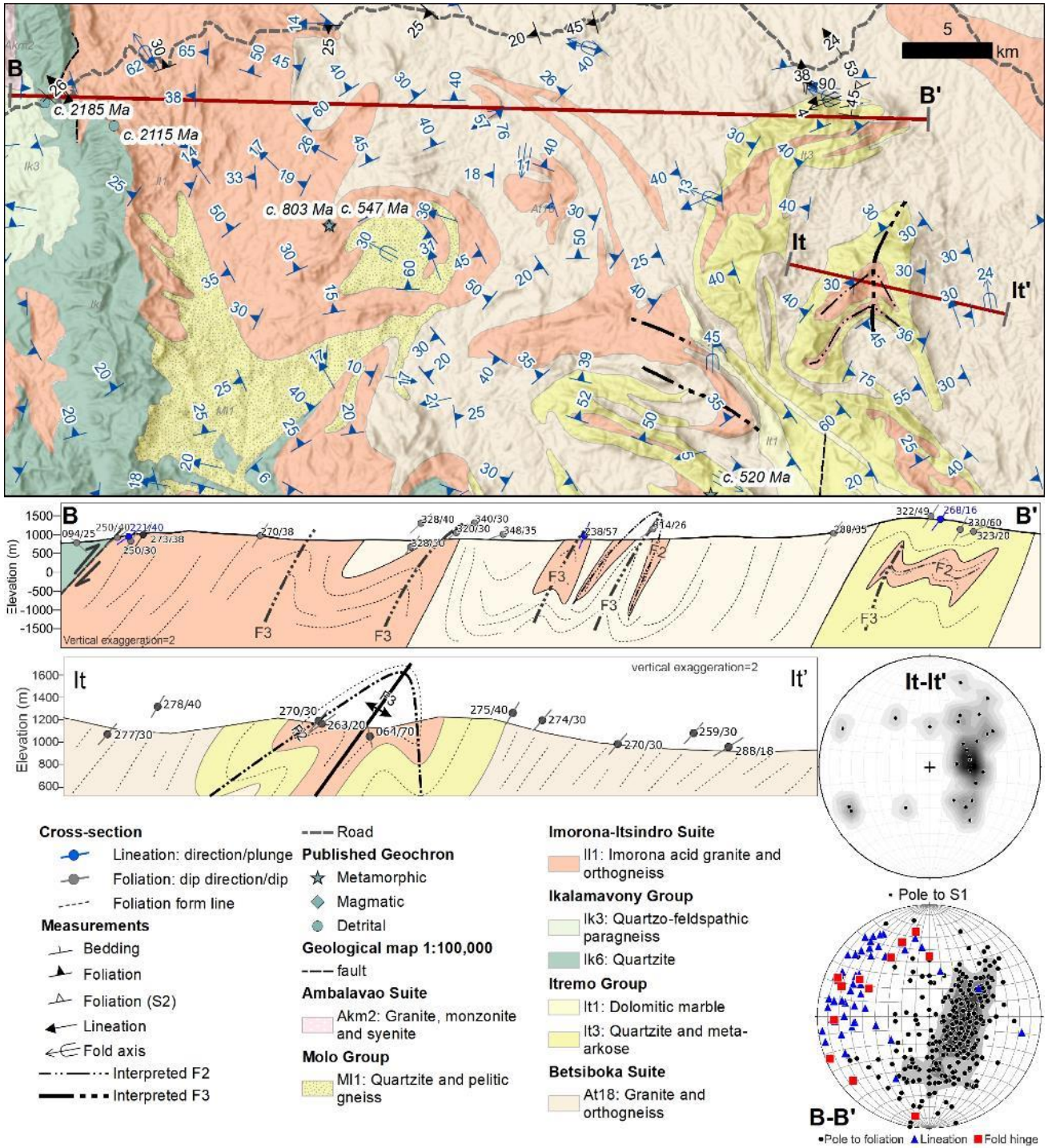
232 2.2. Itremo-Antananarivo Domain

233 The Itremo Group is a continental marginal sequence deposited on basement rocks of the
234 Antananarivo Domain (e.g. Cox et al., 1998; 2004). Therefore, we consider these ‘domains’ together.
235 Transect B–B’ (Figure 5) contains metasedimentary rocks of the Itremo Group, which are dominantly
236 quartzites, marbles and schists, with minor conglomerates. The majority of quartzites that we observe
237 are strongly recrystallised and it is often difficult to recognise primary sedimentary features. The
238 Itremo-Antananarivo Domain was intruded by the c. 850–750 Ma Imorona-Itsindro Suite, after early
239 deformation (Collins et al., 2003b). Together, these suites of rocks underwent a complex deformation
240 history that must post-date the intrusion of the Imorona-Itsindro Suite.

241 Deformation intensity appears to weaken toward the east of the Itremo sub-domain, with an absence of
242 complex fold interference patterns between Antsirabe and Antananarivo. The Imorona-Itsindro Suite
243 in particular becomes progressively less deformed to the east. In the west, the Imorona-Itsindro Suite is
244 folded into fold interference patterns, whereas in the east it only appears to be folded into weakly-
245 defined F3 folds. This is consistent with our sampling of c. 850–750 Ma rocks along this weakly
246 deformed margin (along the main road in Figure 2), where rock samples appear undeformed or very
247 weakly deformed (documented in Table 1).

248 2.2.1. D1 Deformation

249 The orientation of S1 is variable in the Itremo sub-domain due to the abundance of poly-deformed
250 folds. Similar to the Ikalamavony Domain, foliations strike dominantly north-northwest, with
251 lineations and fold axes plunging moderately toward west-northwest. Like the Ikalamavony Domain,
252 the first generation foliation at the outcrop scale is typically defined by the elongation and alignment of
253 biotite, feldspar and quartz in orthogneisses and paragneisses (Figure 6a). In metasedimentary rocks
254 such as quartzites and marbles, the foliation is sometimes defined by the orientation of biotite crystals
255 and biotite rich layers, but is often difficult to recognise due to significant recrystallisation of quartz
256 and a lack of other minerals. Primary sedimentary features such as bedding were difficult to recognise
257 in quartzites due to significant recrystallisation. Within the quartzite packages, there are several
258 conglomerate units with large (up to ~5 cm) pebbles (Figure 6b). Here we observe S0 as the
259 interbedded pebble layers, and S1 as the flattening of pebbles.



260

261 Figure 5 Geological map, structural data and cross-section through the Itremo-Antananarivo Domain using both our new
 262 data and previously published data (Macey et al., 2009). Measured fold axes are generally interpreted to be F2 folds since we
 263 do not observe any overprinting fold generations in the field. Similar to the Ikalamavony transect, the Itremo transect
 264 contains moderately to steeply west-dipping foliations, west-plunging lineations and west to northwest-plunging folds. It-It':
 265 an example of a type 2 fold interference pattern with D2 south-directed recumbent folding overprinted by a F3 north to
 266 north-east trending upright fold. Geological polygons from Council for Geosciences 1:100000 mapsheets (Macey et al.,
 267 2010). Sections generated using QProf plugin in QGIS. Structural measurements (dip direction/dip) within ~2km of the
 268 section are projected along the profile. Topographic profile derived from 30 arc-second DEM of Africa (USGS).

269 2.2.2. *D2 Deformation*

270 Identical to the Ikalamavony Domain, D2 is defined by tight to isoclinal folds with axial traces
271 approximately parallel to S1 in fold limbs. At the outcrop scale we observe these as decimetre- to
272 metre-scale asymmetric, tight to isoclinal folds (Figure 6c,d). F2 folds are similar-type folds, with
273 thickened hinge zones and thinned limbs. F2 axial traces are approximately parallel to S1 at the
274 regional scale. F2 folds are recognisable in remotely sensed data as ~500–1000 m wavelength, tight to
275 isoclinal folds (Figure 5). The original orientation of F2 folds would have had ~east-west striking axial
276 traces, but have been subsequently deformed during D3 and D4. Further south where structures are
277 more north-south trending, Tucker et al. (2007) interpreted east or south-east directed vergence from
278 these fold trends.

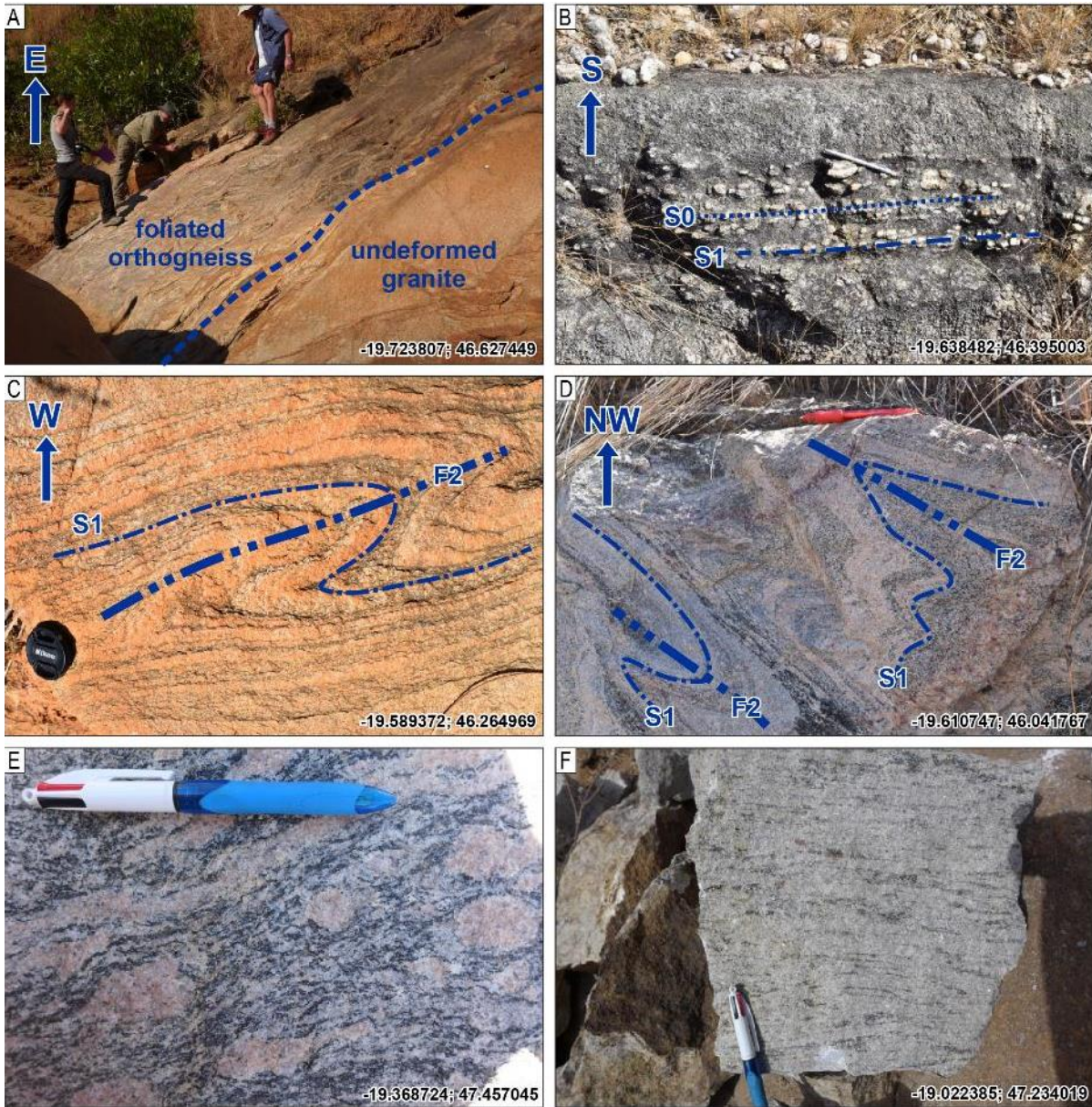
279 2.2.3. *D3 Deformation and associated fold interference patterns*

280 Similar to the Ikalamavony Domain, we do not observe evidence for a third generation deformation
281 event at the outcrop scale, however D3 folds are recognisable in remotely sensed data. The majority of
282 F3 fold axial traces are ~north-south striking, and orthogonally overprint F2 folds. We therefore
283 interpret D3 as an ~east-west shortening event. The folding of F2 folds during D3 has produced a series
284 of fold interference patterns. Type 2 fold interference patterns are observed in remotely sensed data in
285 the Itremo sub-domain (Figure 5).

286 Adding to the complexity of the structure in It-It' is the juxtaposition of older units (the Archean
287 Betsiboka Suite) structurally above younger units (Paleoproterozoic Itremo Group). Tucker et al. (2007)
288 observed that the km-scale fold and thrust nappes (our interpreted D2), resulted in the inversion and
289 repetition of Archean and Proterozoic rocks. This interpretation accounts for why the It-It' section
290 contains older units that appear structurally above younger units.

291 2.2.4. *D4 Deformation*

292 The trend of structures vary from the northwest of central Madagascar near Miandrivazo, to the
293 southeast of the study area along the eastern margin of the Itremo Group (Figure 2). Near Miandrivazo
294 (e.g. Figure 4), F3 axial traces generally trend northwest-southeast. In the Itremo Group and further to
295 the south, these structures are generally north-south trending. This trend broadly follows the curve of
296 our structural style boundary between the western and eastern transects delineated in Figure 3. This
297 regional variation may relate to D4 deformation or may relate to orogenic bending as orogenesis
298 progressed.



299

300 Figure 6 Examples of samples and field outcrops; latitude and longitude given in lower right corner and shown in Figure 2; ,
 301 a) outcrop of foliated gneiss (left) intruded by undeformed granite (right); b) flattened conglomerate where S1 is parallel to
 302 S0 in the Itremo Group of the Itremo sub-domain; c) S1 foliation folded around an F2 fold in the Itremo sub-domain; d) S1
 303 foliation folding around F2 folds in the Itremo sub-domain; e) S1 foliation in a sample of augen gneiss of the Betsiboka Suite
 304 in the Antananarivo Domain; and f) S1 foliation in a sample of gneiss from the Antananarivo Domain, west of Antananarivo.

305 2.3. Antananarivo Domain

306 Precambrian outcrops between Antsirabe and Antananarivo are scarce due to the widespread coverage
 307 of the Ankaratra Volcanics (Figure 2). Generally, deformation in this area is much less intense than the
 308 Ikalamavony Domain and Itremo sub-domain, and we observe fewer deformation events (Figure 7). To
 309 the east of the Antananarivo–Antsirabe road (Figure 2; Figure 7), there is a distinct change in structural
 310 trend. In the Ikalamavony and Itremo domains, structures dominantly trend northwest. North of
 311 Antananarivo, structures trend ~west (approximately the location of Antananarivo virgation zone in
 312 Figure 2), and between Antananarivo and Antsirabe (Figure 7) structures trend ~north. This region was

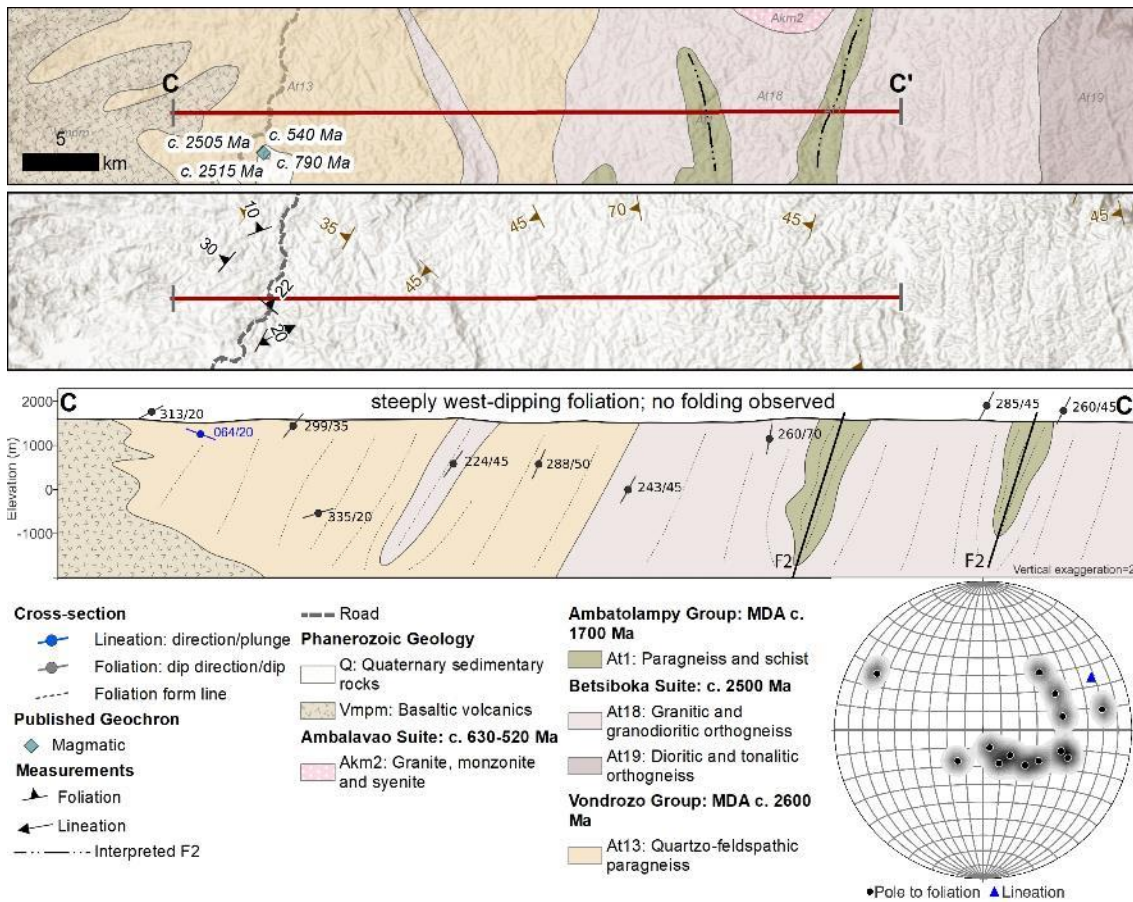
313 studied in detail in Collins et al. (2003a); Nédélec et al. (2000); Raharimahefa and Kusky (2006);
314 Raharimahefa and Kusky (2009); Raharimahefa et al. (2013). The intensity of these structures
315 increases toward the east, with at least four phases of deformation recognised resulting from the
316 Betsimisaraka Suture in eastern Madagascar.

317 *2.3.1. D1 Deformation*

318 Much like the western transect, at the outcrop scale we observe a pervasive foliation within the
319 Betsiboka Suite, which we interpret as an S1 foliation (Figure 6e,f). The foliation is commonly
320 preserved by the alignment of biotite, feldspar and quartz in orthogneisses. Structural measurements
321 indicate that S1 foliations between Antsirabe and Antananarivo dominantly strike ~north-northeast,
322 with dips moderately to the west (Figure 7). North of Antananarivo, S1 is more variable, and folded
323 following the Antananarivo virgation zone (e.g. Nédélec et al., 2000). We observe a well-defined
324 gneissic foliation within the Archean Betsiboka Suite, which may have originally formed prior to
325 Neoproterozoic deformation. If this is the case, then subsequent Neoproterozoic deformation was
326 approximately the same orientation, as we do not observe cross-cutting fabrics.

327 *2.3.2. D2 Deformation*

328 We do not observe D2 structures at the outcrop scale in this section. However, the repetition of
329 mapped Ambatolampy Group within the Betsiboka Suite (Figure 7), indicates that the two elongated
330 Ambatolampy Group bodies in Figure 7 represent tight to isoclinal F2 folds.



331

332

333

334

335

336

Figure 7 Geological map, structural data and cross-section through the Antananarivo Domain. This transect does not contain the complex folding that we observe in the Ikalamavony and Itremo domains. Here, foliations are steeply west-dipping. Geological polygons from Roig et al. (2012). Sections generated using QProf plugin in QGIS. Structural measurements (dip direction/dip) within ~2km of the section are projected along the profile. Topographic profile derived from 30 arc-second DEM of Africa (USGS).

337

3. Thermochronology

338

339

340

341

342

343

344

345

346

347

348

349

350

351

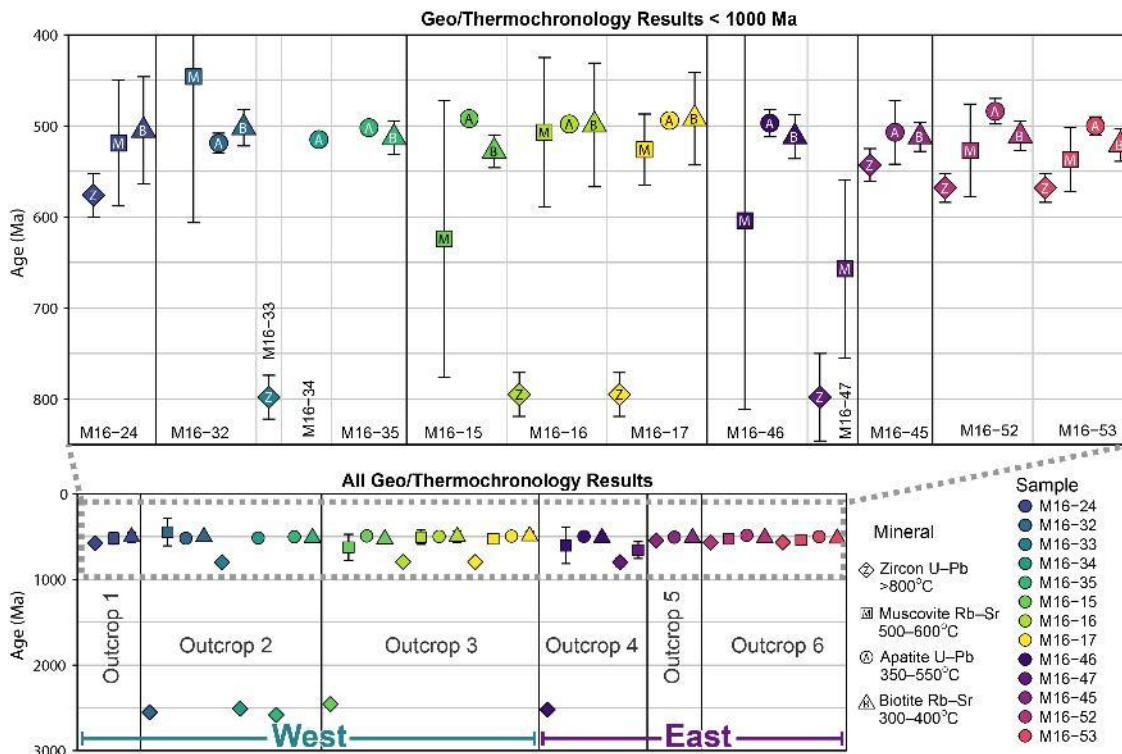
A range of magmatic and orthogneiss samples were collected with the aim of having a representative sample set of the major magmatic suites of central Madagascar. This is important for determining overprinting relationships of key structural events, and determining relative and absolute timing constraints on these events. We used four geochronology/thermochronology techniques: zircon U–Pb (closure temperature ~900–1000°C), apatite U–Pb (closure temperature ~350–550°C), muscovite Rb–Sr (closure temperature ~500–600°C) and biotite Rb–Sr (closure temperature ~300–400°C). The results are summarised in Figure 8 and documented more extensively in Supplementary B. Detailed methodologies for these techniques are also provided in Supplementary B. Rb–Sr mica dating using LA-QQQ-ICP-MS is a novel technique, and this data presents some of the first published data of its kind. The good agreement of Rb–Sr mica ages with U–Pb apatite ages, which have similar closure temperatures, demonstrates that Rb–Sr mica dating is a useful tool for dating medium-temperature events. Due to the abundance of samples (41 in total), detailed results for each sample and outcrop, including plots of isotopic data, are provided in Supplementary B. Sample descriptions, location and age data are summarised in Table 1. Isotopic data are given in Supplementary C.

352
353
354
355

Table 1 Summary of sample descriptions, outcrop and cross-cutting relationships, and age data. Letters given for each outcrop are the interpreted order of formation/intrusion, based on cross-cutting relationships. All zircon ages are interpreted as magmatic crystallisation ages except for metamorphic ages indicated by (*) and lower intercept ages indicated by (#).

Sample ID	Trans ect	Outcrop	Sample description	Magmatic Suite	Latitude	Longitude	Elevation (m)	Zircon U–Pb age (Ma)	Apatite U–Pb age (Ma)	Muscovite Rb–Sr age (Ma)	Biotite Rb–Sr age (Ma)
M16-24	West	1	Undeformed K-feldspar rich granite. Intrudes deformed gabbro interpreted as the Dabolava Suite	Ambalavao	-19.5443	45.47028	182	576 ± 24	–	519 ± 69	505 ± 59
M16-32	West	2/A	Coarse-grained gneiss with 1–2 cm biotite phenocrysts	Betsiboka	-19.6107	46.53399	989	2553 ± 24	519 ± 11	446 ± 161	502 ± 20
M16-33	West	2/D	Undeformed fine-grained granodioritic dyke, intrudes M16-32	Imorona-ltsindro	-19.6107	46.53399	989	798 ± 24	–	–	–
M16-34	West	2/C	Thin dyke intruding M16-32	Betsiboka	-19.6107	46.53399	989	2511 ± 14	515 ± 7	–	–
M16-35	West	2/B	K-feldspar rich deformed dyke	Betsiboka	-19.6107	46.53399	989	2583 ± 26 2494 ± 14 (*)	502 ± 6	–	513 ± 18
M16-15	West	3/A	K-feldspar and biotite rich, foliated orthogneiss	Betsiboka	-19.7239	46.62736	1067	2456 ± 17	492 ± 5	624 ± 152	528 ± 18
M16-16	West	3/B	Undeformed granite, occasionally very weakly foliated	Imorona-ltsindro	-19.7239	46.62736	1067	795 ± 24	498 ± 7	506 ± 82	499 ± 68
M16-17	West	3/C	Pegmatite veins, k-spar rich	Imorona-ltsindro	-19.7239	46.62736	1067	c. 795	494 ± 7	526 ± 39	492 ± 51
M16-46	East	4/A	Foliated orthogneiss, medium-grained, K-feldspar and biotite rich	Betsiboka	-19.1599	47.51211	1351	2522 ± 8 543 ± 27 (#)	497 ± 15	604 ± 211	512 ± 24
M16-47	East	4/B	Undeformed cross-cutting granite	Imorona-ltsindro	-19.1599	47.51211	1351	798 ± 48 532 ± 44 (#)	–	657 ± 98	–
M16-45	East	5	Medium-grained granite, undeformed	Ambalavao	-19.0869	47.54429	1312	543 ± 18	507 ± 35	–	512 ± 16
M16-52	East	6/A	Granite, very weakly foliated	Ambalavao	-18.589	47.23721	1359	568 ± 16	484 ± 14	527 ± 51	511 ± 16
M16-53	East	6/B	Cross-cutting K-feldspar rich granite	Ambalavao	-18.589	47.23721	1359	c. 568	500 ± 10	537 ± 35	521 ± 18

356



357

358

359

360

361

Figure 8 Summary of geo/thermochronology data for each sample and outcrop collected in this study. Error bars are 2σ . Sample locations shown in Figure 2. The bottom figure shows all of the sample data collected, and the top image zooms in on all data that are younger than 1000 Ma. Plots of isotopic data associated with these calculated ages are presented in Supplementary B.

362

4. Discussion

363

4.1. Structural evolution of central Madagascar

364

365

366

367

368

369

370

371

372

The structural style of the Ikalamavony and Itremo domains are indistinguishable and we suggest that D1–D3 (and possibly D4) in both domains were the result of the same orogenic system. Type 1 and type 2 fold interference patterns are common in fold-and-thrust belts, and more commonly form during progressive deformation rather than discrete deformation events. A myriad of complex processes ranging from rheological contrasts to progressive rotation during deformation, commonly cause fold structures with trends that are oblique to the transport direction of the overall fold-and-thrust belt (e.g. Poblet and Lisle, 2011). Therefore, we suggest that D1–D3 in the Ikalamavony Domain and Itremo sub-domain formed during the same orogenic event, through progressive deformation, consistent with the interpretation based on metamorphism in this region by Moine et al. (2014).

373

374

375

376

377

378

A structure with very similar geometry and orientation to the type 2 interference pattern highlighted in Figure 5, was modelled by Armistead et al. (2018). They showed that this type of feature formed from south-directed, tight, recumbent folding that was orthogonally overprinted by third generation upright folding. In our example from the Itremo Group, the F2 recumbent folding formed during south to slightly south-west directed folding that locally formed by ~north-south shortening. The overprinting F3 upright fold formed during ~east-west shortening that resulted in a north to north-east trending

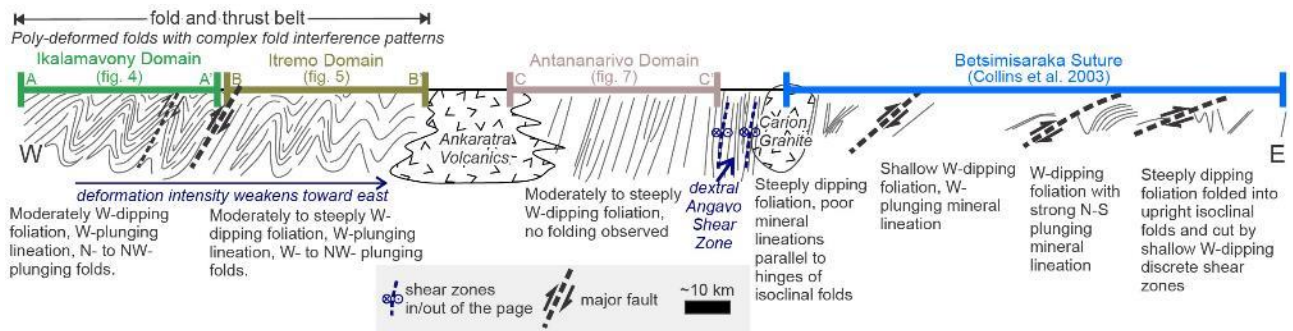
379 axial trace. These interpreted kinematics are consistent with previous interpretations for deformation
380 in the Itremo Group (Collins et al., 2003b; Tucker et al., 2007).

381 As pointed out in Tucker et al. (2007), nappes in the southern Itremo Domain are east-verging and
382 were likely produced within a zone of west-dipping subduction (present day direction). We interpret
383 structures in our study areas of the Ikalamavony and Itremo domains to be dominantly north-west
384 trending, with northeast directed vergence, developed as a result of ~northeast-southwest shortening
385 (present day orientation). We propose that continental collision southwest of the Ikalamavony Domain
386 and Itremo sub-domain was responsible for deformation in central Madagascar. Subduction prior to
387 continental collision was ~southwest dipping.

388 Tucker et al. (2007) proposed that complex folds in the Itremo sub-domain can be broadly considered
389 in two groups; “high-grade, internal nappes” and “low-grade, external nappes.” These were considered
390 to be separated by a west-dipping thrust fault, although the exact location of this boundary is
391 ambiguous from the highly schematic diagrams presented in that study. We broadly agree that
392 metamorphic grade and deformation intensity appears to increase toward the west, however a sharp
393 tectonic boundary hasn’t been observed in this study within the Itremo Group. We do however see a
394 major tectonic boundary between the Ikalamavony Domain and the Itremo-Antananarivo Domain.
395 This boundary may more accurately reflect the boundary between the internal and external nappes
396 proposed by Tucker et al. (2007).

397 The weakly defined, open folding associated with D4 may have occurred in the late stages of folding
398 and thrusting of the Itremo sub-domain and Ikalamavony Domain, or may be related to far-field
399 deformation associated with orogenesis in eastern Madagascar (Collins et al., 2003a).

400 In the eastern part of the study area, east of the ‘structural style boundary’ in Figure 2 and Figure 3, the
401 deformation style changes in orientation and intensity. Transect C–C’ is less deformed than the
402 Ikalamavony and Itremo transects (Figure 9), and we do not observe any complex fold interference
403 patterns here. The orientation of structures also change, and become more north to north-east
404 trending. Further east of our C–C’ transect is the dextral Angavo Shear Zone, which was active at $550 \pm$
405 4 Ma (Raharimahefa and Kusky, 2010). Collins et al. (2003a) constructed a cross-section from
406 Antananarivo eastwards to Brickaville along the east coast of Madagascar (Figure 9). This transect
407 region contains a deformation sequence distinct from the Ikalamavony and Itremo domains and was
408 therefore caused by a different tectonic event. Although controversial, there is significant metamorphic
409 and structural evidence that the sequence of deformation described by Collins et al. (2003a) can be
410 attributed to the c. 550 Ma Betsimisaraka Suture that amalgamated Madagascar with the Dharwar
411 Craton of India.



412

413 Figure 9 Schematic cross-section through central Madagascar from Miandrivazo to Brickaville, combining the cross-sections
 414 of Figure 4, Figure 5, Figure 7 and that of Collins et al. (2003a). The Ikalamavony and Itremo domains preserve the same
 415 structural styles and kinematics. A change in structural style occurs east of these sections, with the Antananarivo Domain
 416 section containing no complex fold interference patterns. Further east, Collins et al. (2003a) interpret intense deformation
 417 associated with the Neoproterozoic–Cambrian Betsimisaraka Suture.

418 4.2. Temporal constraints on deformation

419 4.2.1. Relative timing of deformation

420 Understanding the ages of geological units that are deformed and undeformed can help constrain the
 421 timing of deformation. At the regional scale in the western transect, the c. 850–750 Ma Imorona-
 422 Itsindro Suite is poly-deformed, and therefore was intruded prior to the onset of at least D2 and D3. In
 423 the eastern transect and in the region studied by Collins et al. (2003a); Nédélec et al. (2000);
 424 Raharimahefa and Kusky (2006); Raharimahefa and Kusky (2009), the Imorona-Itsindro Suite is not
 425 poly-deformed into complex fold interference patterns but instead is elongated along the length of the
 426 c. 550 Ma Angavo shear zone (Figure 1b; Figure 9). This indicates that different structural regimes are
 427 responsible for deformation in the west and east of Madagascar.

428 In the Ikalamavony Domain and Itremo sub-domain, the c. 550 Ma Ambalavao Suite is undeformed
 429 and, therefore, provides a minimum age constraint on deformation here. In the east, the Ambalavao
 430 Suite is represented by both deformed and undeformed rocks. We therefore suggest that deformation
 431 in the Ikalamavony Domain and Itremo sub-domain occurred between c. 750 and c. 550 Ma, which is
 432 consistent with interpretations by Tucker et al. (2007). Deformation in eastern Madagascar likely
 433 occurred later at c. 550 Ma, which is consistent with age determinations for the Angavo Shear Zone and
 434 Antananarivo virgation zone (Meert et al., 2003; Nédélec et al., 2000; Paquette and Nédélec, 1998;
 435 Raharimahefa and Kusky, 2010).

436 4.2.2. Thermochronology

437 We have used minerals that record a range of temperatures in an attempt to capture different stages of
 438 the tectonic evolution of Madagascar. Our sampling included the major magmatic suites of
 439 Madagascar, including the c. 2500 Ma Betsiboka Suite, the c. 850–750 Ma Imorona-Itsindro Suite, and
 440 the c. 550 Ma Ambalavao Suite (Figure 8). Interestingly, apatite U–Pb ages—which record the age the
 441 minerals were cooled through ~350–550°C (Chamberlain and Bowring, 2001; Schoene and Bowring,
 442 2007)—are all within a narrow age range from 519 ± 11 Ma to 484 ± 14 Ma, regardless of their
 443 magmatic crystallisation age. Muscovite and biotite, which have Rb–Sr closure temperatures of ~500–

444 600°C (Armstrong et al., 1966) and ~300–400°C (Del Moro et al., 1982; Jenkin et al., 2001; Verschure
445 et al., 1980), respectively, also record ages within a narrow range between 657 ± 98 Ma and 446 ± 161
446 Ma for muscovite (albeit, large uncertainties) and between 528 ± 18 Ma and 492 ± 51 Ma for biotite.
447 This implies that the final stages of orogenesis in Madagascar, regardless of whether this was in the
448 west or east, affected the entire central region of the island, where rocks were either reset to at least
449 ~500°C or cooled through ~500°C at c. 500 Ma.

450 Multiple thermochronometers have provided insights into the medium-temperature thermo-tectonic
451 evolution across the western and eastern part of Madagascar. As we have shown here, the more recent
452 c. 520–480 Ma thermo-tectonic event affected the entire island such that it cooled synchronously
453 through ~500–300°C at c. 500 Ma. The c. 520–480 Ma regional thermal perturbation would have
454 overprinted prior events, obscuring any evidence of a pre-existing thermo-tectonic evolution. Using
455 thermochronometers that record temperatures higher than ~600°C (e.g. monazite U–Pb) in future
456 research may be able to provide further constraints on the timing of orogenesis — particularly in
457 regions distal from the collision zone and in rocks that are not in contact with the Ambalavao Suite —
458 where temperatures during the c. 550 Ma event may not have been hot enough to cause complete reset.
459 Without direct dating of the structures observed, we need to look further afield for evidence of
460 subduction and collision that resulted in deformation of central Madagascar.

461 4.3. Tectonic model for the evolution of central Madagascar

462 The boundaries between the major domains in southern Madagascar represent possible suture zones
463 responsible for deformation in the Ikalamavony Domain and Itremo sub-domain. Prior to the
464 juxtaposition of the Itremo sub-domain and Ikalamavony Domain, we agree with previous
465 interpretations that the Itremo Group was deposited on the Antananarivo Domain basement (Figure
466 10a) (Cox et al., 1998; 2004) and that the Ikalamavony Domain evolved as an exotic island arc terrane
467 (Figure 10b) (Archibald et al., 2017a). The presence of the Imorona-Itsindro Suite in the Ikalamavony
468 Domain indicates that it must have accreted to central Madagascar before c. 850 Ma (Figure 10c). A
469 large west-dipping thrust fault separating the Ikalamavony Domain from the Itremo sub-domain
470 (Figure 5; Figure 9), possibly represents this suture zone (schematic thrust in Figure 10c). This implies
471 west-dipping subduction, which is consistent with previous models for the accretion of the
472 Ikalamavony Domain to central Madagascar (e.g. Boger et al., 2019).

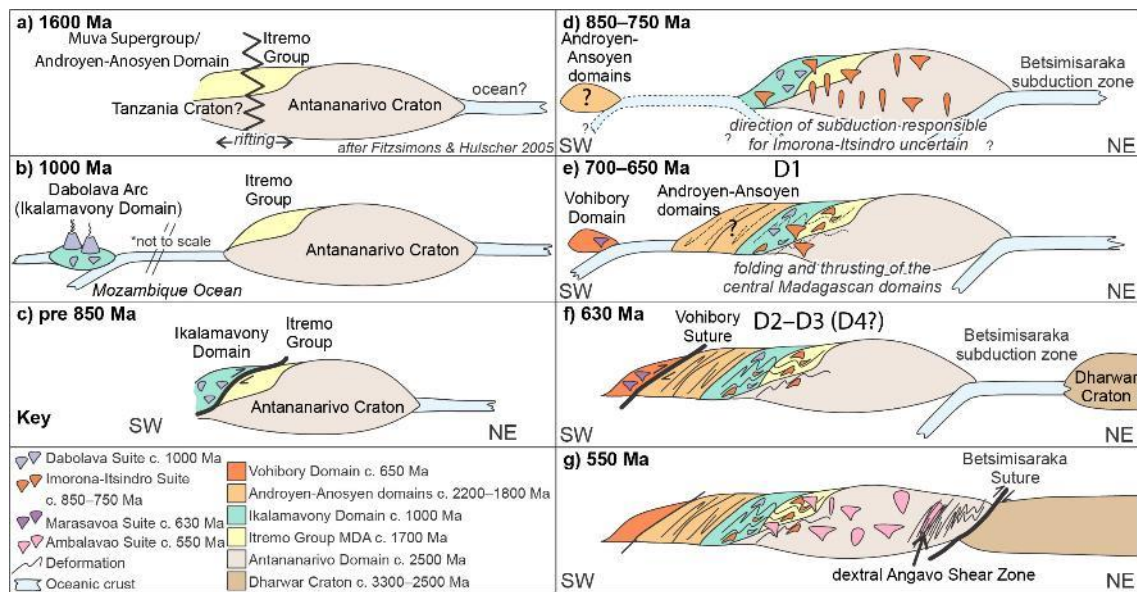
473 Based on the interpreted kinematics and overprinting relationships, deformation of the Ikalamavony
474 Domain and Itremo sub-domain was the result of continental collision. Increasing deformation
475 intensity in the Ikalamavony Domain and the orientation of structures imply that the collision zone
476 must have lain southwest of these domains.

477 Boger et al. (2014); (2019) suggested that the Beraketa high strain zone that separates the Anosyen and
478 Androyen domains represents a c. 580–520 Ma suture. This interpretation was based on c. 630–600 Ma
479 metamorphism restricted to the west of this high-strain zone, and widespread c. 580–520 Ma
480 magmatism and metamorphism on both sides of the high-strain zone. In this model, the subduction
481 zone was east-dipping (present day direction), and resulted in the syn- to post-tectonic Ambalavao
482 granites throughout Madagascar (Figure 10). However, the structures we have described and those

483 described by Tucker et al. (2007) require a ~west-dipping (top to the east; present day direction) sense
484 of movement, making an east-dipping subduction zone beneath the Antananarivo Craton at this time
485 unlikely.

486 These authors interpreted that another west-dipping subduction zone was active beneath the Vohibory
487 Domain until c. 650 Ma (Figure 10e), and that collision between the Vohibory Domain and Androyen
488 Domain occurred at c. 630–610 Ma (Figure 10f), outboard from the Antananarivo Craton (marked by
489 the Ampanihy high-strain zone/Vohibory Suture in Figure 1b). In this model, subduction was west-
490 dipping (Figure 10e,f). Horton et al. (2016) also interpreted that the Androyen and Anosyen domains
491 collided with the Vohibory Domain at c. 630 Ma, based on monazite and zircon geochronology. In our
492 view, this collision zone is most consistent with evidence we see from a structural perspective. We
493 therefore propose that the Vohibory suture was responsible for high intensity deformation and
494 polydeformed folds in the Ikalamaovony and Itremo domains. It's likely that deformation associated
495 with this event is present in the Androyen and Anosyen domains, however structures are much more
496 steeply dipping and more highly strained here, meaning that recognition of distinct folding events is
497 difficult (Figure 10e). As interpreted by Boger et al. (2014); Boger et al. (2019), the Vohibory Suture
498 would have been west-dipping (present day direction), resulting in the emplacement of the c. 630 Ma
499 Marasava Suite in the Vohibory Domain. Metamorphism of this age is also recorded in the Androyen
500 Domain.

501 A change in deformation style and kinematics toward the east of Madagascar and younger
502 geochronological constraints, indicate that complex folding in eastern Madagascar formed in response
503 to a different event than that in the west (Figure 10g). Although we did not look at this region in great
504 detail, the changes across central Madagascar from west to east, combined with extensive structural
505 studies published on eastern Madagascar (Collins et al., 2003a; Martelat et al., 2000; Nédélec et al.,
506 2000; Raharimahefa and Kusky, 2006; Raharimahefa and Kusky, 2009; Raharimahefa et al., 2013),
507 indicate that a west-dipping subduction zone was active at c. 550 Ma, somewhere in the region of the
508 Betsimisaraka Suture.



509

510

511

512

513

514

515

516

517

518

Figure 10 Schematic diagram showing our interpretation of the evolution of central Madagascar. a) Sometime after the deposition of the Itremo Group/Muva Supergroup onto the Antananarivo Craton/Tanzania Craton, these regions begin to rift (Cox et al., 2004; Fitzsimons and Hulscher, 2005); b) at c. 1000 Ma the Dabolava Arc forms as an oceanic island arc outboard from the Antananarivo Domain (Archibald et al., 2017a); c) prior to the intrusion of the c. 850–750 Ma Imorona-Itsindro Suite, the Ikalamavony Domain is thrust over the Antananarivo/Itremo Domain; d) the intrusion of the Imorona-Itsindro Suite resulting from Andean-type subduction, with polarity uncertain (Archibald et al., 2017b); e) west-dipping subduction beneath the Vohibory Domain, with the beginning of deformation (D1); f) closure of the Mozambique ocean along the Vohibory Suture resulting in complex deformation that we have interpreted in central Madagascar (D2–D3) and possibly D4; and g) final amalgamation of central Gondwana along the c. 550 Ma Betsimisaraka Suture.

519

5. Conclusions

520

521

522

523

524

525

526

527

528

529

530

531

We have integrated remote sensing, field data and thermochronology to unravel complex deformation in the Ikalamavony and Itremo domains of central Madagascar. We have recognised four generations (D1–D4) of deformation that resulted in complex fold interference patterns in the Ikalamavony and Itremo domains of central Madagascar. We interpret deformation here as the result of c. 630 Ma collision of Azania with Africa along the Vohibory Suture in southwestern Madagascar. In eastern Madagascar, deformation is syn- to post-550 Ma, which likely formed in response to the final closure of the Mozambique Ocean along the Betsimisaraka Suture that amalgamated Madagascar with the Dharwar Craton of India. Apatite U–Pb and novel LA–QQQ–ICP–MS muscovite and biotite Rb–Sr thermochronology indicate that much of central Madagascar cooled through ~500°C at c. 500 Ma. We have shown the importance of using medium-temperature thermochronometers to date the cooling stages after orogenesis, and the potential for Rb–Sr mica dating to provide useful thermochronological constraints.

532

Acknowledgments

533

534

535

EarthArXiv is thanked for hosting a preprint version of this manuscript, earlier versions of this manuscript can be found there at doi.org/10.31223/osf.io/x46vc. We would like to thank Paul Macey, from the Council for Geoscience, South Africa, for providing additional structural data. Renée Tamblyn

536 is thanked for helpful discussions about Rb–Sr data. We thank Benjamin Emmel, the editor Deta
537 Gasser and two anonymous reviewers for their helpful feedback. This manuscript was also reviewed as
538 part of SA’s PhD thesis by Kathryn Goodenough and Peter Johnson, their valuable feedback greatly
539 improved this manuscript. SA was funded by an Australian government PhD Scholarship and AC is
540 funded by an Australian Research Council Future Fellowship FT120100340. This is a contribution to
541 IGCP projects 628 (Gondwana Map) and 648 (Supercontinent Cycles and Global Geodynamics).

542 References

- 543 Archibald, D.B., Collins, A.S., Foden, J.D., Payne, J.L., Macey, P.H., Holden, P. and Razakamanana, T., 2017a. Stenian–Tonian
544 arc magmatism in west–central Madagascar: the genesis of the Dabolava Suite. *Journal of the Geological Society:*
545 *jgs2017-028*.
- 546 Archibald, D.B., Collins, A.S., Foden, J.D., Payne, J.L., Taylor, R., Holden, P., Razakamanana, T. and Clark, C., 2015. Towards
547 unravelling the Mozambique Ocean conundrum using a triumvirate of zircon isotopic proxies on the Ambatolampy
548 Group, central Madagascar. *Tectonophysics*, 662: 167–182.
- 549 Archibald, D.B., Collins, A.S., Foden, J.D. and Razakamanana, T., 2017b. Tonian Arc Magmatism in Central Madagascar: The
550 Petrogenesis of the Imorona-Itsindro Suite. *The Journal of Geology*, 125(3): 000–000.
- 551 Armistead, S.E., Betts, P.G., Ailleres, L., Armit, R.J. and Williams, H.A., 2018. Cu–Au mineralisation in the Curnamona
552 Province, South Australia: A hybrid stratiform genetic model for Mesoproterozoic IOCG systems in Australia. *Ore*
553 *Geology Reviews*, 94: 104–117.
- 554 Armistead, S.E., Collins, A., Merdith, A.S., Payne, J.L., Cox, G.M., Foden, J.D., Razakamanana, T. and De Waele, B., 2019.
555 Evolving marginal terranes during Neoproterozoic supercontinent reorganisation: constraints from the Bemarivo
556 Domain in northern Madagascar. *Tectonics*.
- 557 Armistead, S.E., Collins, A.S., Payne, J.L., Foden, J.D., De Waele, B., Shaji, E. and Santosh, M., 2017. A re-evaluation of the
558 Kumta Suture in western peninsular India and its extension into Madagascar. *Journal of Asian Earth Sciences*.
- 559 Armstrong, R.L., Jäger, E. and Eberhardt, P., 1966. A comparison of K–Ar and Rb–Sr ages on Alpine biotites. *Earth and*
560 *Planetary Science Letters*, 1(1): 13–19.
- 561 BGS-USGS-GLW, 2008. Republique de Madagascar Ministère de L’energie et des Mines (MEM/SG/DG/UCP/PGRM). British
562 Geological Survey Research Report.
- 563 Boger, S.D., Hirdes, W., Ferreira, C.A.M., Jenett, T., Dallwig, R. and Fanning, C.M., 2015. The 580–520Ma Gondwana suture of
564 Madagascar and its continuation into Antarctica and Africa. *Gondwana Research*, 28(3): 1048–1060.
- 565 Boger, S.D., Hirdes, W., Ferreira, C.A.M., Schulte, B., Jenett, T. and Fanning, C.M., 2014. From passive margin to volcano–
566 sedimentary forearc: The Tonian to Cryogenian evolution of the Anosyen Domain of southeastern Madagascar.
567 *Precambrian Research*, 247: 159–186.
- 568 Boger, S.D., Maas, R., Pastuhov, M., Macey, P.H., Hirdes, W., Schulte, B., Fanning, C.M., Ferreira, C.A.M., Jenett, T. and
569 Dallwig, R., 2019. The tectonic domains of southern and western Madagascar. *Precambrian Research*.
- 570 Chamberlain, K.R. and Bowring, S.A., 2001. Apatite–feldspar U–Pb thermochronometer: a reliable, mid-range (~450°C),
571 diffusion-controlled system. *Chemical Geology*, 172(1): 173–200.
- 572 Collins, A.S., 2006. Madagascar and the amalgamation of Central Gondwana. *Gondwana Research*, 9(1–2): 3–16.
- 573 Collins, A.S., Fitzsimons, I.C.W., Hulscher, B. and Razakamanana, T., 2003a. Structure of the eastern margin of the East
574 African Orogen in central Madagascar. *Precambrian Research*, 123(2–4): 111–133.
- 575 Collins, A.S., Johnson, S., Fitzsimons, I.C., Powell, C.M., Hulscher, B., Abello, J. and Razakamanana, T., 2003b.
576 Neoproterozoic deformation in central Madagascar: a structural section through part of the East African Orogen.
577 Geological Society, London, Special Publications, 206(1): 363–379.
- 578 Collins, A.S., Kinny, P.D. and Razakamanana, T., 2012. Depositional age, provenance and metamorphic age of
579 metasedimentary rocks from southern Madagascar. *Gondwana Research*, 21(2–3): 353–361.
- 580 Collins, A.S., Kröner, A., Fitzsimons, I.C.W. and Razakamanana, T., 2003c. Detrital footprint of the Mozambique ocean: U–
581 Pb SHRIMP and Pb evaporation zircon geochronology of metasedimentary gneisses in eastern Madagascar.
582 *Tectonophysics*, 375(1–4): 77–99.
- 583 Collins, A.S. and Pisarevsky, S.A., 2005. Amalgamating eastern Gondwana: The evolution of the Circum-Indian Orogens.
584 *Earth-Science Reviews*, 71(3–4): 229–270.
- 585 Collins, A.S., Razakamanana, T. and Windley, B.F., 2000. Neoproterozoic extensional detachment in central Madagascar:
586 implications for the collapse of the East African Orogen. *Geological Magazine*, 137(1): 39–51.
- 587 Collins, A.S. and Windley, B.F., 2002. The tectonic evolution of central and northern Madagascar and its place in the final
588 assembly of Gondwana. *The Journal of Geology*, 110(3): 325–339.
- 589 Cox, R., Armstrong, R.A. and Ashwal, L.D., 1998. Sedimentology, geochronology and provenance of the Proterozoic Itremo
590 Group, central Madagascar, and implications for pre-Gondwana palaeogeography. *Journal of the Geological Society*,
591 155(6): 1009–1024.

592 Cox, R., Coleman, D.S., Chokel, C.B., DeOreo, S.B., Wooden, J.L., Collins, A.S., De Waele, B. and Kröner, A., 2004.
593 Proterozoic tectonostratigraphy and paleogeography of central Madagascar derived from detrital zircon U-Pb age
594 populations. *The Journal of geology*, 112(4): 379-399.

595 De Waele, B., Thomas, R.J., Macey, P.H., Horstwood, M.S.A., Tucker, R.D., Pitfield, P.E.J., Schofield, D.I., Goodenough, K.M.,
596 Bauer, W., Key, R.M., Potter, C.J., Armstrong, R.A., Miller, J.A., Randriamananjara, T., Ralison, V., Rafahatelo, J.M.,
597 Rabarimanana, M. and Bejoma, M., 2011. Provenance and tectonic significance of the Palaeoproterozoic
598 metasedimentary successions of central and northern Madagascar. *Precambrian Research*, 189(1-2): 18-42.

599 de Wit, M.J., Bowring, S.A., Ashwal, L.D., Randrianasolo, L.G., Morel, V.P.I. and Rambeloson, R.A., 2001. Age and tectonic
600 evolution of Neoproterozoic ductile shear zones in southwestern Madagascar, with implications for Gondwana
601 studies. *Tectonics*, 20(1): 1-45.

602 Del Moro, A., Puxeddu, M., di Brozolo, F.R. and Villa, I.M., 1982. Rb-Sr and K-Ar ages on minerals at temperatures of 300°-
603 400° C from deep wells in the Larderello geothermal field (Italy). *Contributions to Mineralogy and Petrology*, 81(4):
604 340-349.

605 Emmel, B., Jons, N., Kroner, A., Jacobs, J., Wartho, J.A., Schenk, V., Razakamanana, T. and Austegard, A., 2008. From Closure
606 of the Mozambique Ocean to Gondwana Breakup: New Evidence from Geochronological Data of the Vohibory
607 Terrane, Southwest Madagascar. *The Journal of Geology*, 116(1): 21-38.

608 Fernandez, A., Schreurs, G., Villa, I.M., Huber, S. and Rakotondrazafy, M., 2003. Age constraints on the tectonic evolution of
609 the Itremo region in Central Madagascar. *Precambrian Research*, 123(2-4): 87-110.

610 Fitzsimons, I.C.W. and Hulscher, B., 2005. Out of Africa: detrital zircon provenance of central Madagascar and
611 Neoproterozoic terrane transfer across the Mozambique Ocean. *Terra Nova*, 17(3): 224-235.

612 Grasmann, B., Wiesmayr, G., Draganits, E. and Füsseis, F., 2004. Classification of re-fold structures. *The Journal of geology*,
613 112(1): 119-125.

614 Horton, F., Hacker, B., Kylander-Clark, A., Holder, R. and Jöns, N., 2016. Focused radiogenic heating of middle crust caused
615 ultrahigh temperatures in southern Madagascar. *Tectonics*, 35(2): 293-314.

616 Jenkin, G.R.T., Ellam, R.M., Rogers, G. and Stuart, F.M., 2001. An investigation of closure temperature of the biotite Rb-Sr
617 system: The importance of cation exchange. *Geochimica et Cosmochimica Acta*, 65(7): 1141-1160.

618 Jöns, N., Emmel, B., Schenk, V. and Razakamanana, T., 2009. From orogenesis to passive margin—the cooling history of the
619 Bemarivo Belt (N Madagascar), a multi-thermochronometer approach. *Gondwana Research*, 16(1): 72-81.

620 Jöns, N. and Schenk, V., 2008. Relics of the Mozambique Ocean in the central East African Orogen: evidence from the
621 Vohibory Block of southern Madagascar. *Journal of Metamorphic Geology*.

622 Jöns, N. and Schenk, V., 2011. The ultrahigh temperature granulites of southern Madagascar in a polymetamorphic context:
623 implications for the amalgamation of the Gondwana supercontinent. *European Journal of Mineralogy*, 23(2): 127-
624 156.

625 Kröner, A., Hegner, E., Collins, A.S., Windley, B.F., Brewer, T.S., Razakamanana, T. and Pidgeon, R.T., 2000. Age and
626 magmatic history of the Antananarivo Block, central Madagascar, as derived from zircon geochronology and Nd
627 isotopic systematics. *American Journal of Science*, 300(4): 251-288.

628 Macey, P.H., Bisnath, A., Yibas, B., Robson, L. and Andriamanantsoa, E., 2009. *Carte Géologique de Madagascar*, Council for
629 Geoscience, Pretoria, Afrique du Sud.

630 Macey, P.H., Thomas, R.J., Grantham, G.H., Ingram, B.A., Jacobs, J., Armstrong, R.A., Roberts, M.P., Bingen, B., Hollick, L.,
631 de Kock, G.S., Viola, G., Bauer, W., Gonzales, E., Bjerkgård, T., Henderson, I.H.C., Sandstad, J.S., Cronwright, M.S.,
632 Harley, S., Solli, A., Nordgulen, Ø., Motuza, G., Daudi, E. and Manhiça, V., 2010. Mesoproterozoic geology of the
633 Nampula Block, northern Mozambique: Tracing fragments of Mesoproterozoic crust in the heart of Gondwana.
634 *Precambrian Research*, 182(1-2): 124-148.

635 Martelat, J.-E., Lardeaux, J.-M., Nicollet, C. and Rakotondrazafy, R., 2000. Strain pattern and late Precambrian deformation
636 history in southern Madagascar. *Precambrian research*, 102(1-2): 1-20.

637 Meert, J.G., Nédélec, A. and Hall, C., 2003. The stratoid granites of central Madagascar: paleomagnetism and further age
638 constraints on neoproterozoic deformation. *Precambrian Research*, 120(1-2): 101-129.

639 Meredith, A.S., Collins, A.S., Williams, S.E., Pisarevsky, S., Foden, J.D., Archibald, D.B., Blades, M.L., Alessio, B.L., Armistead,
640 S. and Plavsá, D., 2017. A full-plate global reconstruction of the Neoproterozoic. *Gondwana Research*, 50: 84-134.

641 Moine, B., 1968. *Massif Schisto-Quartzo-Dolomitique: Reion d'Ambatofinandrahana centre-ouest du socle cristallin
642 précambrien de Madagascar* In: N. Sciences de la terre (Editor). Centre de l'Institut Géographique National à
643 Tananarive.

644 Moine, B., Bosse, V., Paquette, J.-L. and Ortega, E., 2014. The occurrence of a Tonian–Cryogenian (~850Ma) regional
645 metamorphic event in Central Madagascar and the geodynamic setting of the Imorona–Itsindro (~800Ma)
646 magmatic suite. *Journal of African Earth Sciences*, 94: 58-73.

647 Nédélec, A., Ralison, B., Bouchez, J.L. and Grégoire, V., 2000. Structure and metamorphism of the granitic basement around
648 Antananarivo: A key to the Pan-African history of central Madagascar and its Gondwana connections. *Tectonics*,
649 19(5): 997-1020.

650 Paquette, J.-L. and Nédélec, A., 1998. A new insight into Pan-African tectonics in the East–West Gondwana collision zone by
651 U–Pb zircon dating of granites from central Madagascar. *Earth and Planetary Science Letters*, 155(1-2): 45-56.

652 Paquette, J.-L., Nédélec, A., Moine, B. and Rakotondrazafy, M., 1994. U-Pb, single zircon Pb-evaporation, and Sm-Nd isotopic
653 study of a granulite domain in SE Madagascar. *The Journal of Geology*, 102(5): 523-538.

- 654 Poblet, J. and Lisle, R.J., 2011. Kinematic evolution and structural styles of fold-and-thrust belts. Geological Society, London,
655 Special Publications, 349(1): 1-24.
- 656 Raharimahefa, T. and Kusky, T.M., 2006. Structural and remote sensing studies of the southern Betsimisaraka Suture,
657 Madagascar. *Gondwana Research*, 10(1-2): 186-197.
- 658 Raharimahefa, T. and Kusky, T.M., 2009. Structural and remote sensing analysis of the Betsimisaraka Suture in northeastern
659 Madagascar. *Gondwana Research*, 15(1): 14-27.
- 660 Raharimahefa, T. and Kusky, T.M., 2010. Temporal evolution of the Angavo and related shear zones in Gondwana:
661 Constraints from LA-MC-ICP-MS U-Pb zircon ages of granitoids and gneiss from central Madagascar. *Precambrian
662 Research*, 182(1-2): 30-42.
- 663 Raharimahefa, T., Kusky, T.M., Toraman, E., Rasoazanamparany, C. and Rasaonina, I., 2013. Geometry and kinematics of the
664 late Proterozoic Angavo Shear Zone, Central Madagascar: Implications for Gondwana Assembly. *Tectonophysics*,
665 592: 113-129.
- 666 Roig, J., Tucker, R., Delor, C., Peters, S. and Théveniaut, H., 2012. Carte géologique de la République de Madagascar à 1/1 000
667 000, Ministère des Mines, PGRM, Antananarivo, République de Madagascar.
- 668 Schoene, B. and Bowring, S.A., 2007. Determining accurate temperature-time paths from U-Pb thermochronology: An
669 example from the Kaapvaal craton, southern Africa. *Geochimica et Cosmochimica Acta*, 71(1): 165-185.
- 670 Schofield, D.I., Thomas, R.J., Goodenough, K.M., De Waele, B., Pitfield, P.E.J., Key, R.M., Bauer, W., Walsh, G.J., Lidke, D.J.
671 and Ralison, A.V., 2010. Geological evolution of the Antongil Craton, NE Madagascar. *Precambrian Research*, 182(3):
672 187-203.
- 673 Service Géologique de Madagascar, T., 1962. Moramanga-Brickaville.
- 674 Service Géologique de Madagascar, T., 1963a. Antsirabe-Ampatolampy
- 675 Service Géologique de Madagascar, T., 1963b. Miarinarivo-Tanarive.
- 676 Thomas, R.J., De Waele, B., Schofield, D.I., Goodenough, K.M., Horstwood, M., Tucker, R., Bauer, W., Annells, R., Howard,
677 K., Walsh, G., Rabarimanana, M., Rafahatelo, J.M., Ralison, A.V. and Randriamananjara, T., 2009. Geological
678 evolution of the Neoproterozoic Bemarivo Belt, northern Madagascar. *Precambrian Research*, 172(3-4): 279-300.
- 679 Tucker, R., Ashwal, L., Handke, M., Hamilton, M., Le Grange, M. and Rambeloson, R., 1999. U-Pb geochronology and isotope
680 geochemistry of the Archean and Proterozoic rocks of north-central Madagascar. *The Journal of Geology*, 107(2):
681 135-153.
- 682 Tucker, R., Roig, J.-Y., Delor, C., Amelin, Y., Goncalves, P., Rabarimanana, M., Ralison, A. and Belcher, R., 2011.
683 Neoproterozoic extension in the Greater Dharwar Craton: a reevaluation of the "Betsimisaraka suture" in
684 Madagascar. *Canadian Journal of Earth Sciences*, 48(2): 389-417.
- 685 Tucker, R.D., Kusky, T.M., Buchwaldt, R. and Handke, M.J., 2007. Neoproterozoic nappes and superposed folding of the
686 Itremo Group, west-central Madagascar. *Gondwana Research*, 12(4): 356-379.
- 687 Tucker, R.D., Roig, J.Y., Moine, B., Delor, C. and Peters, S.G., 2014. A geological synthesis of the Precambrian shield in
688 Madagascar. *Journal of African Earth Sciences*, 94: 9-30.
- 689 Verschure, R.H., Andriessen, P.A.M., Boelrijk, N.A.I.M., Hebeda, E.H., Maijer, C., Priem, H.N.A. and Verdurmen, E.A.T.,
690 1980. On the thermal stability of Rb-Sr and K-Ar biotite systems: Evidence from coexisting Sveconorwegian (ca 870
691 Ma) and Caledonian (ca 400 Ma) biotites in SW Norway. *Contributions to Mineralogy and Petrology*, 74(3): 245-
692 252.
- 693